PHYSICAL REVIEW D **95,** 056023 (2017)

Probing the diffractive production of a *Z*-boson pair at forward rapidities at the LHC

Hao Sun*

Institute of Theoretical Physics, School of Physics, Dalian University of Technology, No. 2 Linggong Road, Dalian, Liaoning 116024, People's Republic of China

(Received 21 February 2017; published 29 March 2017)

In this paper, we present the results from phenomenological analysis of *Z*-boson pair hard diffractive production at the LHC. The calculation is based on the Regge factorization approach. Diffractive parton density functions extracted by the H1 Collaboration at DESY-HERA are used. The multiple Pomeron exchange corrections are considered through the rapidity gap survival probability factor. We give numerical predictions for single diffractive as well as double Pomeron exchange cross sections and compare with the photon-induced and nondiffractive ones. The contributions from quark-antiquark collision and gluon-gluon fusion are displayed. Various kinematical distributions are presented. We make predictions which could be compared to future measurements at the LHC, where forward proton detectors are installed and detector acceptances are considered.

DOI: 10.1103/PhysRevD.95.056023

I. INTRODUCTION

Hadronic processes can be classified as being either soft or hard, where soft (hard) means strong interaction processes with a small (large) momentum transfer. The hard sector is well described by perturbative quantum chromodynamics (pQCD), where the coupling constant (α_s) is small (compared to the "hard" momentum transfer) and a perturbative expansion in terms proportional to powers of α_s works. This is done by means of QCD factorization [1,2] which has been thoroughly tested and taken as the most powerful tool in describing high-energy hadronic collisions. On the other hand, soft processes are characterized by an energy scale of the order of the hadron size ($1\ \text{fm} \simeq 200\ \text{MeV}$) where α_s is large enough to make the higher-order terms non-negligible, thus making the soft processes intrinsically nonperturbative. To gain an understanding of soft or nonperturbative QCD, it is therefore advantageous to first consider soft effects in hard scattering events since the hard scale gives a firm ground in terms of a parton-level process which is calculable in pQCD. This hard-soft interplay is the basis for the research field of diffractive hard scattering.

Encoding the parton distribution functions (PDFs), one can separate the hard perturbation contributions from the soft nonperturbative ones. Following this idea, factorization is still being used and has been carefully proved in diffractive deep inelastic scattering (DDIS) [3]. In the framework of Regge factorization, the so-called Ingelman and Schlein (IS) model [4] has been largely used in describing hard diffractive events in electron-proton (ep) collisions [5]. The IS model essentially considers that diffractive scattering is attributed to the exchange of a Pomeron, i.e. a colorless object with vacuum quantum numbers. The Pomeron is treated like a real particle, and one considers that a diffractive ep collision is due to an electron-Pomeron collision and that a diffractive proton-proton (pp) collision is due to a proton-Pomeron collision. However, the nature of the Pomeron and its reaction mechanisms are still unknown. Diffractive study may help us understanding more about the QCD Pomeron structure. One should be careful that factorization seems to be broken when going from DDIS at HERA to hadron-hadron collisions at the Tevatron and the Large hadron collider (LHC). Theoretical studies [6] predicted that the breakdown of the factorization is due to soft rescattering corrections associated to reinteractions (referred to as multiple scatterings effects) between spectator partons of the colliding hadrons that fill in the rapidity gaps related to Pomeron exchange.

In order to constrain the modeling of the gap survival effects and also improve our limited understanding of diffraction, it will be crucial to, in experimental point of view, discriminate the diffractive production from the nondiffractive processes. Indeed, diffractive events can be characterized by having a rapidity gap (RG), say, a region in rapidity or polar angle without any particles. Another definition is to require a leading particle carrying most of the beam particle momentum, which is kinematically related to a RG. These RGs in the forward or backward rapidity regions, connect directly to the soft part of the events, and therefore nonperturbative effects, on a long spacetime scale. Thus, the experimental signature for diffractive production is either the presence of one(two) RG(s) in the detector or one(both) proton(s) tagged in the final state(s). The potential for using RG vetoes to select diffractive events are highly favored by the newly installed HERSCHEL forward detectors [7] at LHCb, due to its low

*haosun@mail.ustc.edu.cn; haosun@dlut.edu.cn

instantaneous luminosity and wide rapidity coverage. Similar scintillation counters are also installed at ALICE [8] and CMS [7]. Potentially intact proton(s) tagging to select(or exclude) exclusive(or diffractive) events can be realized by using the approved AFP [9] and installed CT-PPS [10] forward proton spectrometers, associated with the ATLAS and CMS central detectors [11] at the LHC. The installation of forward detectors at the LHC may provide possibility, somehow open a new window to study new physics at TeV scale, whereas diffractive events may serve as one of the most important background source. Besides Regge factorization or the amount of gap survival probability which are widely accepted approximations, resonance production, in the central and forward (proton excitation) regions, is also an important issue. Related studies can be found, i.e., in refs [12–14]. In any case, diffractive productions worth being carefully studied and precisely estimated.

A lot of works on diffraction can be found in the literatures for a long time which include, i.e., diffractive dijet [4], heavy flavor jets [15–17], Drell-Yan pair [18], photon [19] and also diffractive Higgs productions [20–25], etc. In our present paper, we concentrate on the hard diffractive Z-boson pair production at the LHC. Diffractive hadroproduction of single electroweak boson was first observed experimentally at the Tevatron [26]. Theoretical analysis were presented in [27–30] at the Tevatron, in [31] at the RHIC, and in [31–35] at the LHC. Typically, ref. [33] show that single diffractive W boson production asymmetry in rapidity is a particularly good observable at the LHC to test the concept of the flavor symmetric Pomeron parton distributions and may provide an additional constraint for the PDFs in the proton. Ref. [34] show that diffractive gauge bosons production can be useful to constrain the modeling of the gap survival effects. All these referees show that by using gauge boson productions, studies of the Pomeron structure and diffraction phenomenology are feasible. For diboson production, diffractive W boson pair is the frontier one which have been studied in refs. [36,37]. The Z-boson pair diffractive is less important due to its small production rate compare to W boson pair production. Nevertheless, at the LHC high-energy frontier, still worth being studied rather than at the Tevatron.

Our paper is organized as follows: in Sec. II, we present the production mechanisms starting from general production to diffractive ones. We show the details concerning the parametrization for the diffractive PDFs in the Pomeron. In addition, we present the theoretical estimations for the gap survival probability factor. Typically, the forward detector acceptances are considered. We present our numerical results and perform predictions to future measurements at the LHC in Sec. III. Finally, we present our summary in the last section.

II. CALCULATION FRAMEWORK

A. Production Mechanism

Our starting point is the introduction of the general inclusive total cross section for the process

$$p_1 + p_2 \to (a + b \to Y) + X \tag{1}$$

in Fig. 1(a), in which partons of two hadrons (a from p_1 and b from p_2) interact to produce a Y system, at the center of mass (CMS) energy $\sqrt{s}$. The total hadronic inclusive cross section is obtained by convoluting the total partonic cross section with the PDFs of the initial hadrons,

$$\sigma_{p_1p_2\to Y+X}(s,\mu_F^2,\mu_R^2) = \sum_{a,b=q,\bar{q},g}\int_{\tau_0}^1 2zdz\int_{z^2}^1\frac{dx_1}{x_1}f_{a/p_1}(x_1,\mu_F^2)f_{b/p_2}\left(\frac{z^2}{x_1},\mu_F^2\right)\hat{\sigma}_{a+b\to Y}(\hat{s}=z^2s,\mu_F^2,\mu_R^2)+(a\rightleftharpoons b) \tag{2}$$

where the sum $a, b = q, \bar{q}, g$ is over all massless partons. $z^2 = x_1x_2$ with x_1 and x_2 are the hadron momentum fractions carried by the interacting partons. The partonic cross section is $\hat{\sigma}_{a+b\to Y}(\hat{s},\mu_F^2,\mu_R^2)$, where $\hat{s}$ is the partonic CMS energy, $\mu_F(\mu_R)$ is the renormalization(factorization) scale, $\tau_0 = m_Y/\sqrt{s}$ and m_Y is the mass threshold for the Y system, $f_{i/p}(x_i,\mu_F^2)$ is the PDF of a parton of flavor i in the hadron p and are evaluated at the factorization scale

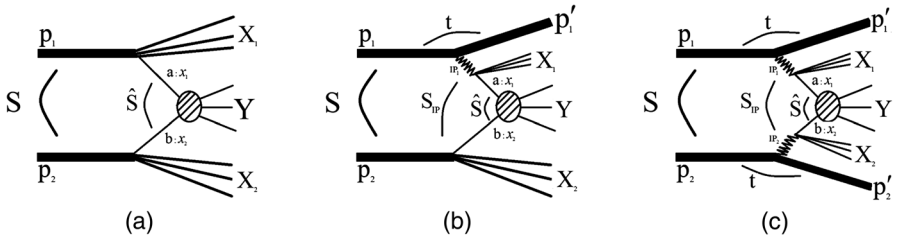

FIG. 1. Illustrated diagrams for the nondiffractive (a), single diffractive (b) and double Permon exchange (c) production.

(usually assumed to be equal to the renormalization scale).

For the hard diffractive processes, we will consider the Ingelman-Schlein (IS) picture [4], in which a Pomeron structure (with quark and gluon content) is introduced. In the expression for single diffractive (SD) processes, there includes three steps: First, one of the hadrons, say hadron p_1 with energy E, emits a Pomeron ($\mathbb{P}_1$), with only a small squared four-momentum transfer $|t|$, and turns to hadron p_1' with energy E' but remains almost intact. Second, the remaining hadron scatters off the emitted Pomeron. Partons from the Pomeron interact with partons from the other hadron (p_2) and produce a Y system. Finally, hadron p_1' is detected in the final state with a reduced energy loss (defined as $\xi = (E - E')/E$) by proposed forward proton detectors [9,10]. Meantime, the Y system and the remaining remnants (X) go to the general central detectors. A typical SD reaction is presented in Fig. 1(b) and can be given as

$$p_1 + p_2 \to p_1 + (a + b \to Y) + X. \tag{3}$$

In the IS approach, the SD cross section is assumed to factorize into the total Pomeron-hadron cross section and a Pomeron flux factor [4]. This means we can replace the PDFs in Eq. (2) by

$$x_i f_{i/p}(x_i,\mu^2) \Rightarrow x_i f^D_{i/p}(x_i,\mu^2) = \int dx_{\mathbb{P}} \int d\beta \bar{f}(x_{\mathbb{P}}) \cdot \beta f_{i/\mathbb{P}}(\beta,\mu^2) \cdot \delta\left(\beta - \frac{x_i}{x_{\mathbb{P}}}\right) \equiv \int dx_{\mathbb{P}} \bar{f}(x_{\mathbb{P}}) \frac{x_i}{x_{\mathbb{P}}} f_{i/\mathbb{P}}\left(\frac{x_i}{x_{\mathbb{P}}},\mu^2\right), \tag{4}$$

with the defined quantity $\bar{f}(x_{\mathbb{P}}) \equiv \int_{t_{\min}}^{t_{\max}} f_{\mathbb{P}/p}(x_{\mathbb{P}}, t)dt$. Here $\beta f_{i/\mathbb{P}}(\beta,\mu^2)$ is the PDF of a parton of flavor i in the Pomeron and $f_{\mathbb{P}/p}(x_{\mathbb{P}}, t)$ is the Pomeron flux factor, describe the emission rate of Pomerons by the hadron. $x_{\mathbb{P}}$ is the Pomeron kinematical variable defined as $x_{\mathbb{P}} = s_{\mathbb{P}_1 p_2}/s_{p_1 p_2}$, where $\sqrt{s_{\mathbb{P}_1 p_2}}$ is the CMS energy in the Pomeron-hadron system and $\sqrt{s_{p_1 p_2}} \equiv \sqrt{s}$ is the CMS energy in the hadron (p_1) hadron (p_2) system. The single diffractive cross section can be written as

$$\begin{aligned}
\sigma^{\mathrm{SD}}_{p_1 p_2 \to p_1 + Y + X}(s,\mu_F^2,\mu_R^2) &= \sum_{a,b=q,\bar{q},g} \int_{\tau_0}^1 2z dz \int_{z^2}^1 \frac{dx_1}{x_1} f^D_{a/p_1}(x_1,\mu_F^2) f_{b/p_2}\left(\frac{z^2}{x_1},\mu_F^2\right) \\
\hat{\sigma}_{a+b\to Y}(\hat{s} = z^2 s,\mu_F^2,\mu_R^2) + (a \rightleftharpoons b) &= \sum_{a,b=q,\bar{q},g} \int_{\tau_0}^1 2z dz \int_{z^2}^1 \frac{dx_1}{x_1} \int_{x_1}^{x_{\mathbb{P}}^{\max}} \frac{dx_{\mathbb{P}}}{x_{\mathbb{P}}} \bar{f}_{\mathbb{P}/p_1}(x_{\mathbb{P}}) f_{a/\mathbb{P}}\left(\frac{x_1}{x_{\mathbb{P}}},\mu_F^2\right) f_{b/p_2}\left(\frac{z^2}{x_1},\mu_F^2\right) \\
&\quad \times \hat{\sigma}_{a+b\to Y}(\hat{s} = z^2 s,\mu_F^2,\mu_R^2) + (a \rightleftharpoons b).
\end{aligned} \tag{5}$$

A similar factorization can also be applied to double Pomeron exchange (DPE) process, where both colliding hadrons can be detected in the final states. This diffractive process is also known as central diffraction (CD) production. The illustration diagram is presented in Fig. 1(c). A typical DPE reaction is given as

$$p_1 + p_2 \to p_1 + (a + b \to Y) + X + p_2. \tag{6}$$

The total cross section for DPE processes reads as

$$\begin{aligned}
\sigma^{\mathrm{DPE}}_{p_1 p_2 \to p_1 + Y + X + p_2}(s,\mu_F^2,\mu_R^2) &= \sum_{a,b=q,\bar{q},g} \int_{\tau_0}^1 2z dz \int_{z^2}^1 \frac{dx_1}{x_1} f^D_{a/p_1}(x_1,\mu_F^2) f^D_{b/p_2}\left(\frac{z^2}{x_1},\mu_F^2\right) \hat{\sigma}_{a+b\to Y}(\hat{s} = z^2 s,\mu_F^2,\mu_R^2) \\
&= \sum_{a,b=q,\bar{q},g} \int_{\tau_0}^1 2z dz \int_{z^2}^1 \frac{dx_1}{x_1} \int_{x_1}^{x_{\mathbb{P}_1}^{\max}} \frac{dx_{\mathbb{P}_1}}{x_{\mathbb{P}_1}} \bar{f}_{\mathbb{P}_1/p_1}(x_{\mathbb{P}_1}) f_{a/\mathbb{P}_1}\left(\frac{x_1}{x_{\mathbb{P}_1}},\mu_F^2\right) \\
&\quad \times \int_{z^2/x_1}^{x_{\mathbb{P}_2}^{\max}} \frac{dx_{\mathbb{P}_2}}{x_{\mathbb{P}_2}} \bar{f}_{\mathbb{P}_2/p_2}(x_{\mathbb{P}_2}) f_{b/\mathbb{P}_2}\left(\frac{z^2}{x_1 x_{\mathbb{P}_2}},\mu_F^2\right) \hat{\sigma}_{a+b\to Y}(\hat{s} = z^2 s,\mu_F^2,\mu_R^2).
\end{aligned} \tag{7}$$

B. The Pomeron structure function

In order to estimate the diffractive cross sections, two elements are needed:

(i) $f_{i/\mathbb{P}}(x_i, \mu^2)$: the diffractive parton distribution function (dPDF) which describe a perturbative distribution of partons in the Pomeron. We will consider the dPDFs extracted by the H1 collaboration at DESY-HERA [38].

(ii) $f_{\mathbb{P}/p}(x_{\mathbb{P}}, t)$: the Pomeron flux factor which describe the "emission rate" of Pomeron by the hadron and represents the probability that a Pomeron with particular values of $(x_{\mathbb{P}}, t)$ couples to the proton.

The dPDFs are modeled in terms of a light flavor singlet distribution $\Sigma(z)$, consisting of u, d and s quarks and antiquarks with $u = d = s = \bar{u} = \bar{d} = \bar{s}$, and a gluon distribution $g(z)$. Here z is the longitudinal momentum fraction of the parton entering the hard subprocess with respect to the diffractive exchange, such that $z = \beta$ for the lowest-order quark-parton model process, whereas $0 < \beta < z$ for higher-order processes. The quark singlet and gluon distributions are parametrized at Q_0^2 using the general form

$$z f_i(z, Q_0^2) = A_i z^{B_i} (1-z)^{C_i} \exp\left[-\frac{0.01}{1-z}\right], \tag{8}$$

where the last exponential factor ensures that the dPDF's vanish at $z = 1$, as required for the evolution equations to be solvable. For the quark singlet distribution, the data require the inclusion of all three parameters A_q, B_q and C_q in Eq. (8). By comparison, the gluon density is weakly constrained by the data, which is found to be insensitive to the B_g parameter. The gluon density is thus parametrized at Q_0^2, using only the A_g and C_g parameters. With this parametrization, one has the value $Q_0^2 = 1.75$ GeV^2 and it is referred to as the "H1 2006 dPDF Fit A." It is verified that the fit procedure is not sensitive to the gluon PDF and a new adjustment was made with $C_g = 0$. Thus, the gluon density is then a simple constant at the starting scale for evolution, which was chosen to be $Q_0^2 = 2.5$ GeV^2 and it is referred to as the "H1 2006 dPDF Fit B."

For the Pomeron flux factor, we apply the standard flux form from Regge phenomenology [39], based on the Donnachie-Landshoff model [40,41]. The $x_{\mathbb{P}}$ dependence is parametrized by

$$f_{\mathbb{P}/p}(x_{\mathbb{P}}, t) = A_{\mathbb{P}} \cdot \frac{e^{B_{\mathbb{P}} t}}{x_{\mathbb{P}}^{2\alpha_{\mathbb{P}}(t)-1}}, \tag{9}$$

where the Pomeron Regge trajectory is assumed to be linear, $\alpha_{\mathbb{P}}(t) = \alpha_{\mathbb{P}}(0) + \alpha'_{\mathbb{P}} t$, and the parameters $B_{\mathbb{P}}$ and $\alpha'_{\mathbb{P}}$ and their uncertainties are obtained from fits to H1 FPS data [42]. In our calculation, we take $\alpha_{\mathbb{P}}(0) = 1.1182 \pm 0.008$ in fit A ($\alpha_{\mathbb{P}}(0) = 1.1110 \pm 0.007$ in fit B), $B_{\mathbb{P}} = 5.5^{-2.0}_{+0.7}$ GeV^{-2} and $\alpha'_{\mathbb{P}} = 0.06^{+0.19}_{-0.06}$ GeV^{-2}. The value of the normalization parameter $A_{\mathbb{P}}$ is chosen such that $x_{\mathbb{P}} \cdot \int_{t_{\min}}^{t_{\max}} f_{\mathbb{P}/p}(x_{\mathbb{P}}, t) dt = 1$ at $x_{\mathbb{P}} = 0.003$, where $t_{\max} \simeq -\frac{m_p^2 x_{\mathbb{P}}^2}{1-x_{\mathbb{P}}}$ is the maximum kinematically accessible value of t, $m_p = 0.93827231$ GeV is the proton mass and $t_{\min} = -1.0$ GeV^2 is the limit of the measurement. So we get

$$A_{\mathbb{P}} = \frac{x_{\mathbb{P}}^{2\alpha_{\mathbb{P}}(0)-2}(B_{\mathbb{P}} - 2\alpha'_{\mathbb{P}} \ln x_{\mathbb{P}})}{\exp\left[-(B_{\mathbb{P}} - 2\alpha'_{\mathbb{P}} \ln x_{\mathbb{P}}) \frac{m_p^2 x_{\mathbb{P}}^2}{1-x_{\mathbb{P}}}\right] - \exp[-(B_{\mathbb{P}} - 2\alpha'_{\mathbb{P}} \ln x_{\mathbb{P}})]} \quad \text{with} \quad x_{\mathbb{P}} = 0.003. \tag{10}$$

Thus, we have

$$\bar{f}(x_{\mathbb{P}}) = \frac{A_{\mathbb{P}}}{x_{\mathbb{P}}^{2\alpha_{\mathbb{P}}(0)-1}(B_{\mathbb{P}} - 2\alpha'_{\mathbb{P}} \ln x_{\mathbb{P}})} \cdot \left[\exp\left[-(B_{\mathbb{P}} - 2\alpha'_{\mathbb{P}} \ln x_{\mathbb{P}}) \frac{m_p^2 x_{\mathbb{P}}^2}{1-x_{\mathbb{P}}}\right] - \exp[-(B_{\mathbb{P}} - 2\alpha'_{\mathbb{P}} \ln x_{\mathbb{P}})]\right]. \tag{11}$$

C. Multiple-Pomeron scattering corrections

We have assumed Regge factorization which is known to be violated in hadron-hadron collisions. Theoretical studies predicted that the violation is due to the soft interactions between spectator partons of the colliding hadrons, which lead to an extra production of particles that fill in the rapidity gaps related to Pomeron exchange. So that when the rapidity gaps are measured, one has to include absorption effect in the formalism of the resolved Pomeron. Different models of absorption corrections (one-, two- or three-channel approaches) for diffractive processes were presented in the literature. The absorption effects for the diffractive processes were calculated e.g. in [43–45]. The different models give slightly different predictions. Usually, an average value of the gap survival probability $\langle |S|^2 \rangle$ is calculated first and then the cross sections for different processes is multiplied by this value. Here we shall follow this simplified approach. The survival probability depends on the collision energy and can be sometimes parametrized as

$$\langle|S|^2\rangle(\sqrt{s}) = \frac{a}{b + \ln(\sqrt{s/s_0})}, \tag{12}$$

with a $= 0.126$, $b = -4.688$ and $s_0 = 1$ GeV^2 and more details can be found in original publications. This formula gives the typical values of survival probabilities for diffractive production in proton-proton collisions of 4.5% at Tevatron and 2.6% at the LHC. Indeed, more precise values should be updated by measurements. For example, from the diffractive cross sections at the 8 TeV LHC, one gets typically value of $\langle|S|^2\rangle = 8\%$ extracted by the CMS collaboration for diffractive dijet production [46]. For the SD production and DPE production, there should be some difference for the value of the factors. The probable uncertainty may be as large as 30%, which is one of the largest uncertainty sources in diffractive production and should able to be reduced thanks to the forthcoming measurements at the LHC.

D. Forward detector acceptance

We assume the intact protons in diffractive events to be tagged in the forward proton detectors of the CMS-TOTEM Collaborations [10], or those to be installed by the ATLAS Collaboration in the future called AFP detectors [9]. The idea is to measure scattered protons at very small angles at the interaction point and to use the LHC magnets as a spectrometer to detect and measure them. We use the following acceptances [47]:

(i) $0.015 < \xi < 0.15$ for ATLAS-AFP
(ii) $0.0001 < \xi < 0.17$ for TOTEM-CMS.

These acceptances correspond to cuts on longitudinal momentum fractions of outgoing protons. To obtain the constrained diffractive PDFs, we convolute the Pomeron flux with the Pomeron PDFs while imposing a reduction in the phase space of ξ. Imaging a reduced energy loss can be probed in the range $\xi_{\min} < \xi < \xi_{\max}$, we can write the final ξ dependent SD cross section as [48]

$$\sigma^{\rm SD}_{p_1p_2\to p_1+Y+X}(s,\mu_F^2,\mu_R^2) = \langle|S|^2\rangle_{\rm SD}\sum_{a,b=q,\bar{q},g}\int_{\tau_0}^1 2zdz\int_{z^2}^1\frac{dx_1}{x_1}\int_{{\rm Max}(x_1,\xi_{\min})}^{{\rm Min}(x_{\mathbb{P}}^{\max},\xi_{\max})}\frac{dx_{\mathbb{P}}}{x_{\mathbb{P}}}\bar{f}_{\mathbb{P}/p_1}(x_{\mathbb{P}})f_{a/\mathbb{P}}\left(\frac{x_1}{x_{\mathbb{P}}},\mu_F^2\right)$$
$$\times f_{b/p_2}\left(\frac{z^2}{x_1},\mu_F^2\right)\hat{\sigma}_{a+b\to Y}(\hat{s}=z^2s,\mu_F^2,\mu_R^2) + (a\rightleftharpoons b) \tag{13}$$

The final cross section for the DPE processes can be written as [48]

$$\sigma^{\rm DPE}_{p_1p_2\to p_1+Y+X+p_2}(s,\mu_F^2,\mu_R^2) = \langle|S|^2\rangle_{\rm DPE}\sum_{a,b=q,\bar{q},g}\int_{\tau_0}^1 2zdz\int_{z^2}^1\frac{dx_1}{x_1}\int_{{\rm Max}(x_1,\xi_{\min})}^{{\rm Min}(x_{\mathbb{P}_1}^{\max},\xi_{\max})}\frac{dx_{\mathbb{P}_1}}{x_{\mathbb{P}_1}}\bar{f}_{\mathbb{P}_1/p_1}(x_{\mathbb{P}_1})f_{a/\mathbb{P}_1}\left(\frac{x_1}{x_{\mathbb{P}_1}},\mu_F^2\right)$$
$$\times\int_{{\rm Max}(z^2/x_1,\xi_{\min})}^{{\rm Min}(x_{\mathbb{P}_2}^{\max},\xi_{\max})}\frac{dx_{\mathbb{P}_2}}{x_{\mathbb{P}_2}}\bar{f}_{\mathbb{P}_2/p_2}(x_{\mathbb{P}_2})f_{b/\mathbb{P}_2}\left(\frac{z^2}{x_1x_{\mathbb{P}_2}},\mu_F^2\right)\hat{\sigma}_{a+b\to Y}(\hat{s}=z^2s,\mu_F^2,\mu_R^2). \tag{14}$$

III. NUMERICAL RESULTS

At parton level, Z pair hadronic production is induced by quark–antiquark collision mode at the leading order (LO). For gluon-gluon (and $\gamma\gamma$ fusion for photoproduction) fusion initial state, the LO contribution is induced at the one-loop level due to the missing of the tree contribution. We perform our numerical calculations with in-house coding based on FeynArts, FormCalc and LoopTools (FFL) package [49–51]. We adopt BASES [52] to do the phase space integration. In what follows, we present predictions for hard diffractive production of a Z-boson pair based on previous discussion.

In Fig. 2, we show the invariant mass distributions of the diffractive Z boson pair production at the 14 TeV LHC. We compare contributions of single diffractive (first panel) and double Pomeron exchange processes (second panel). The SD distributions are larger than that of the DPE production by a factor of 20 without considering the absorption factor. We also present the subcontributions from the up-antiup quark collision (dash-dotted curve), down-antidown quark collision (dotted curve) as well as gluon-gluon fusion (dashed curve). In any case down-quark collision dominates among the different contributions. Their sum is plot by the solid curve. As we said, the calculation is done assumes Regge factorization. Absorption corrections can be taken into account by a multiplicative factor being a probability of a rapidity gap survival [see e.g. Eq. (12)]. Such a factor is approximately $\langle|S|^2\rangle = 0.03$ for the LHC energy $\sqrt{s} = 14$ TeV. The diffractive distributions in the figure should be multiplied in addition by these factors. In order to avoid model dependence, the reader can use his/her own number when comparing different contributions. Here and in the following the absorption effects are not included for simplicity.

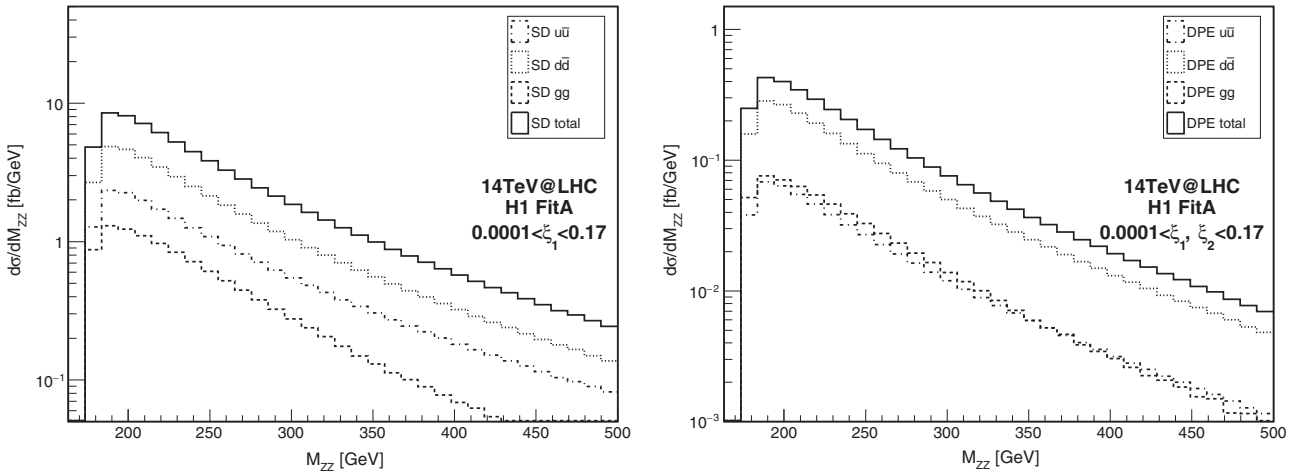

FIG. 2. The invariant mass distribution for the diffractive Z-boson pair production at the 14 TeV LHC. Here we use "H1 2006 dPDF Fit A". $0.0001 < \xi < 0.17$ for TOTEM-CMS is considered. Absorption effects are not included here.

In Fig. 3, we present the Z transverse momentum distribution in the first two panels for SD and DPE production, respectively. As can be seen, its kinematically allowed range extend up to around half of $M_{ZZ}^{\max}$. Given the fast-falling nature of the M_{ZZ} distribution, dominated by low values of the invariant, the Z boson transverse momentum distribution shows a maximum at $p_T \sim M_{ZZ}^{\min}/4$. The rapidity distribution of the Z boson is shown in the second two panels. Both the SD and DPE contribution as well as subcontributions are concentrated at midrapidities and strongly asymmetric around $y = 0$ as a consequence of limiting integration over $x_{\mathbb{P}}$ in the range $0.0001 < \xi < 0.17$.

In Fig. 4 we present the $x_{\mathbb{P}}$ distribution for single diffractive Z-boson pair production. Still, TOTEM-CMS detector acceptance is considered for simplicity. We show the up-quark collision, the down-quark collision and the gluon-gluon fusion productions separately and use solid curve to present their total sum as the function of $x_{\mathbb{P}}$. As displayed in the figure, the dominant contribution come from the down-quark collision which is around 2 to 4 times larger than that of the others. For the up-quark collision and gluon-gluon fusion, their contributions discrepant largely in the small range of $x_{\mathbb{P}}$, while become close to each other as the value of $x_{\mathbb{P}}$ become larger. Typically, the quark collision contribution enhance obviously at the small $x_{\mathbb{P}}$ range, say, approximately as an inverse power of $x_{\mathbb{P}}$ at small $x_{\mathbb{P}}$. This is not the same as in the gluon-gluon fusion case where there is some suppression at the small value of $x_{\mathbb{P}}$. Nevertheless, the total contribution still show obvious enhancement at small $x_{\mathbb{P}}$ range.

In order to compare, we display the same distribution in Fig. 5 for double Pomeron exchange Z-boson pair production. $x_{\mathbb{P}}$ is one fraction of the proton side (first panel). As can be found in the figure, in contrast with the SD production, $x_{\mathbb{P}}$ DPE distribution decreases at small $x_{\mathbb{P}}$ range for both the quark-collision and the gluon-gluon fusion. In order to include the fraction distribution for both sides of the proton in the DPE production, we define $x'_{\mathbb{P}} = \sqrt{x^2_{\mathbb{P}_1} + x^2_{\mathbb{P}_2}}$ and display its distribution in the second panel in Fig. 5. It will be interesting to find out that $x'_{\mathbb{P}}$ distribution spread mainly in the central range while on both bound ranges, decreases to small values. For the front range may due to the large mass of Z-boson pair causes that the small value of $x_{\mathbb{P}_{1,2}}$ are not accessible kinematically, while the behavior in the ending boundary is due to the forward detector acceptance we considered that makes a behavior of the strong suppression.

The first uncertainty in diffractive productions is the gap survival probability as we mentioned above. Another error represents the propagation of experimental uncertainties is obtained in the diffractive PDF fit. We show this in Fig. 6 and Fig. 7 for SD and DPE production. Results of 8, 13 TeV and distributions of $x_{\mathbb{P}}$ and rapidity are presented as examples. The detector acceptance is fixed in the range of $0.0001 < \xi_1 < 0.17$ where similar results can be obtained for $0.015 < \xi_1 < 0.15$. The "H1 2006 dPDF Fit A" (solid curves) is considered, whereas a replacement by "H1 2006 dPDF Fit B" (dotted curves) keeps the results slightly different. For the PDFs in the proton we have always considered the cteq6L1 parametrization [53]. As can be seen, the discrepancy induced by using different fits in DPE production is a little larger than that in SD production. For all $x_{\mathbb{P}}$, $\sqrt{x^2_{\mathbb{P}_1} + x^2_{\mathbb{P}_2}}$ and rapidity distributions, the small enhancement showed mainly at the peak range. Nevertheless, there is no large discrepancy observed, therefore, the uncertainty is small in using the different fit procedures for diffractive PDFs.

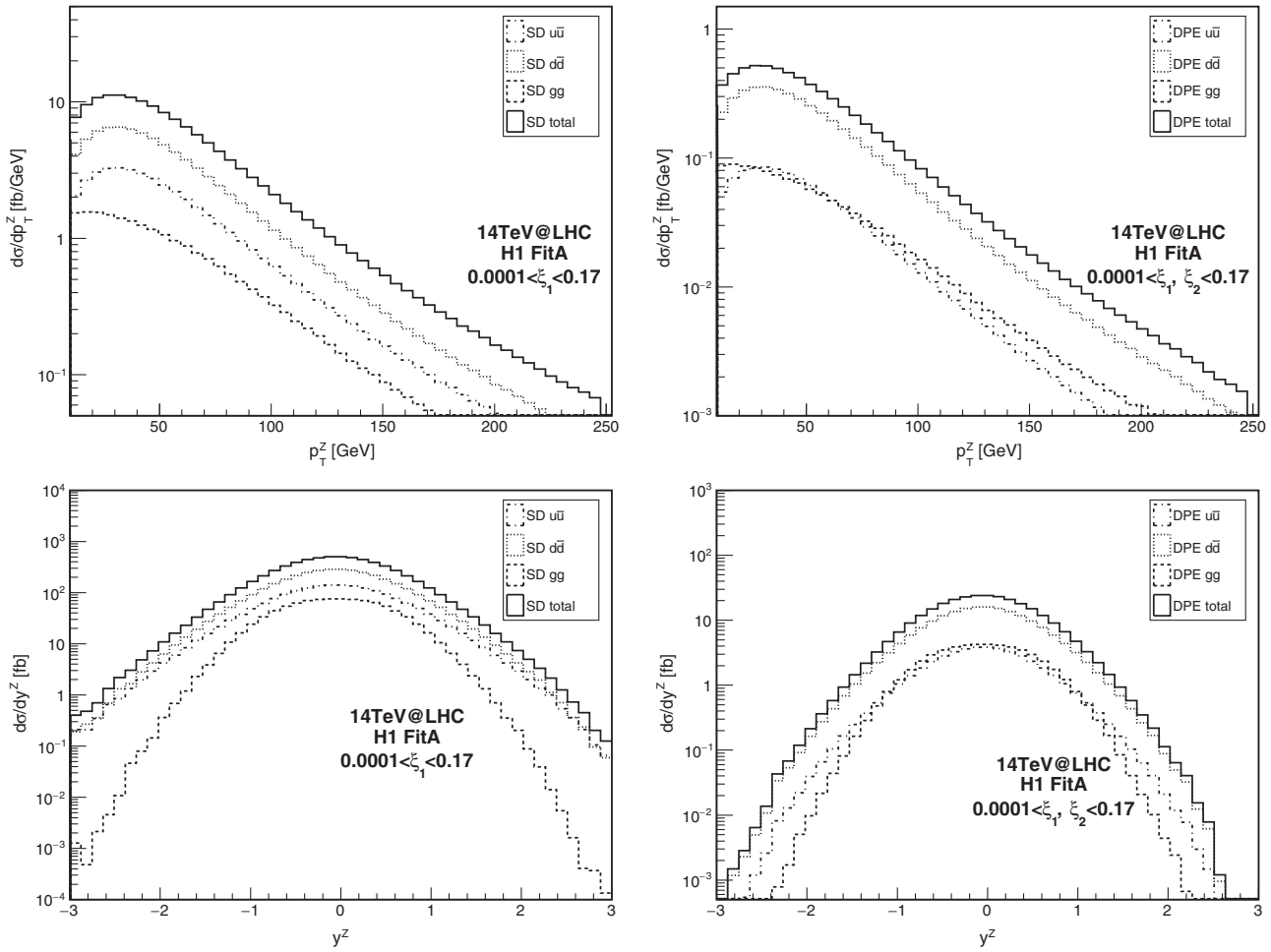

FIG. 3. The transverse momentum and rapidity distributions for the Z boson at the 14 TeV LHC. Here we use "H1 2006 dPDF Fit A". $0.0001 < \xi < 0.17$ for TOTEM-CMS is considered. Absorption effects are not included here.

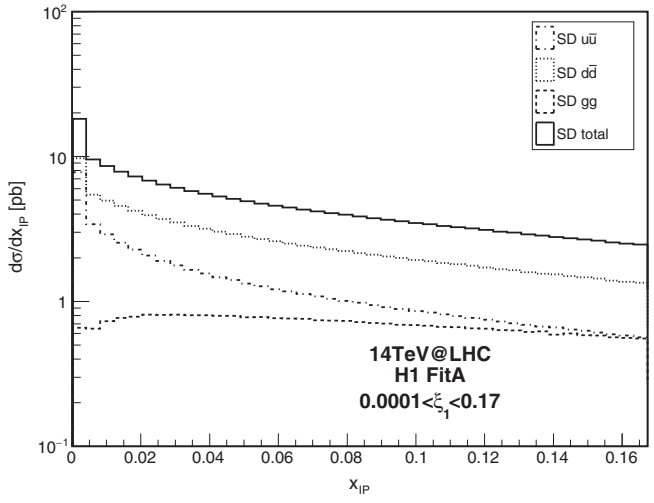

FIG. 4. The $x_{\mathbb{P}}$ distribution for single diffractive (SD) Z-boson pair production at the 14 TeV LHC. Here we use "H1 2006 dPDF Fit A". $0.0001 < \xi < 0.17$ for TOTEM-CMS is considered. Absorption effects are not included here.

The third uncertainty, of theoretical nature, is obtained by varying the factorization scales. Such uncertainties can be reduced by including higher-order corrections, whereas the complete calculation is out of the scope here. In the present content, we stabilize against factorization scale variation conveniently by considering appropriate ratios of diffractive over nondiffractive (ND) cross sections

$$R = \frac{\sigma(pp \to pYX)}{\sigma(pp \to YX)} \quad \text{and} \quad R = \frac{\sigma(pp \to pYXp)}{\sigma(pp \to YX)}, \quad (15)$$

or DPE cross section over the SD ones

$$R = \frac{\sigma(pp \to pYXp)}{\sigma(pp \to pYX)}, \quad (16)$$

which also offer the advantage to reduce experimental systematics errors. Here Y stands for the selected hard scattering process (Z-boson pair in this case) and X for the unobserved part of the final states. At the Tevatron, the ratio R has been measured in a variety of final states [54–56] and

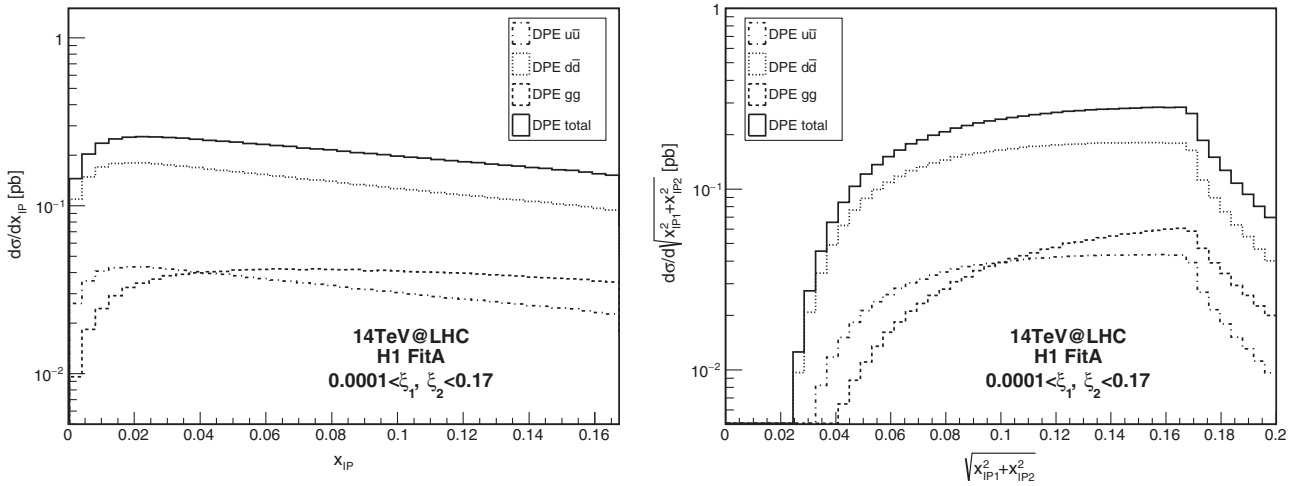

FIG. 5. The $x_{\mathbb{P}}$ ($x'_{\mathbb{P}}$) distribution for double Pomeron exchange (DPE) Z-boson pair production at the 14 TeV LHC. $0.0001 < \xi < 0.17$ for TOTEM-CMS is considered. Absorption effects are not included here.

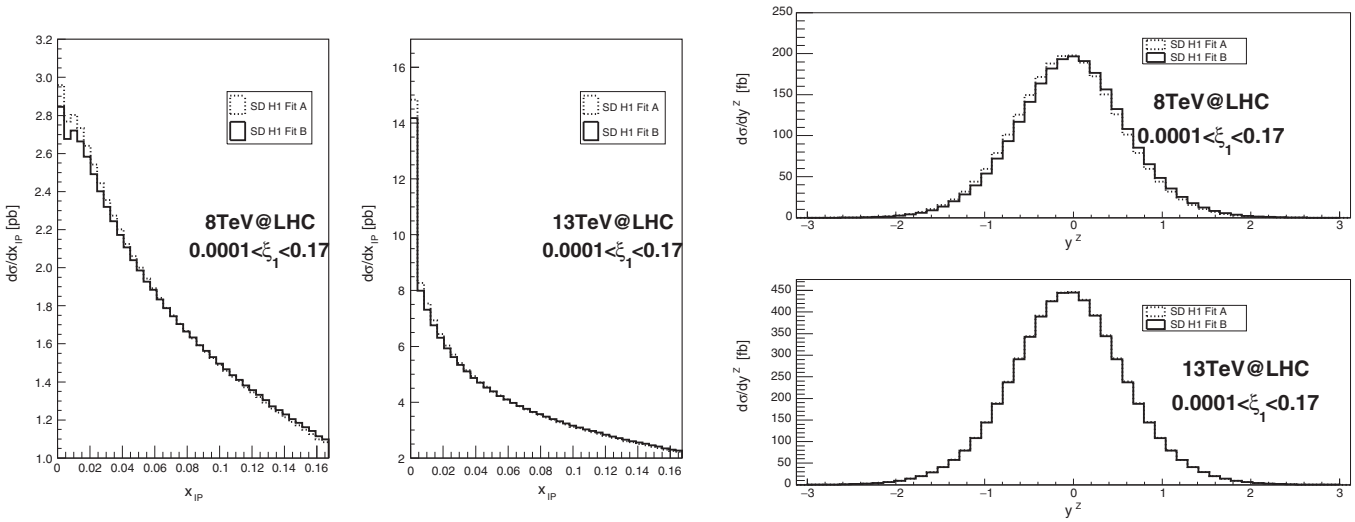

FIG. 6. Single diffractive (SD) production of $x_{\mathbb{P}}$ and rapidity distributions at the 8 and 13 TeV LHC with the use of "H1 2006 dPDF Fit A" (solid curves) and "H1 2006 dPDF Fit B" (dotted curves). The detector acceptances are fixed in the range of $0.0001 < \xi_1 < 0.17$. Absorption effects are not included here.

show some stable behavior with a value close to one percent. Typically, in our case considering at the distribution level, we define the single diffractive ratio as

$$R_1 = \frac{d\sigma_{\mathrm{SD}}}{d\sigma_{\mathrm{ND}}}, \tag{17}$$

the double Permon diffractive ratio by

$$R_2 = \frac{d\sigma_{\mathrm{DPE}}}{d\sigma_{\mathrm{ND}}}, \tag{18}$$

and, also, the DPE over SD ratio as

$$R_3 = \frac{d\sigma_{\mathrm{DPE}}}{d\sigma_{\mathrm{SD}}}. \tag{19}$$

As predicted in Fig. 8, we plot the R ratio as a function of M_{ZZ} distribution with solid curve for R_1, dashed curve for R_2 and dotted curve for R_3, respectively. Based on these results, we verify that, for the single diffractive Z-boson pair production in pp collision, given the leading-order estimate of the nondiffractive cross section, the ratio R_1 is varies between 5% and 7% and decreases mildly as a function of the invariant mass of the Z boson pair. The double Pomeron exchange productions are about 20–100 times smaller than that of the single diffractive ones, as can be found in the DPE over SD ratio R_3, varies between

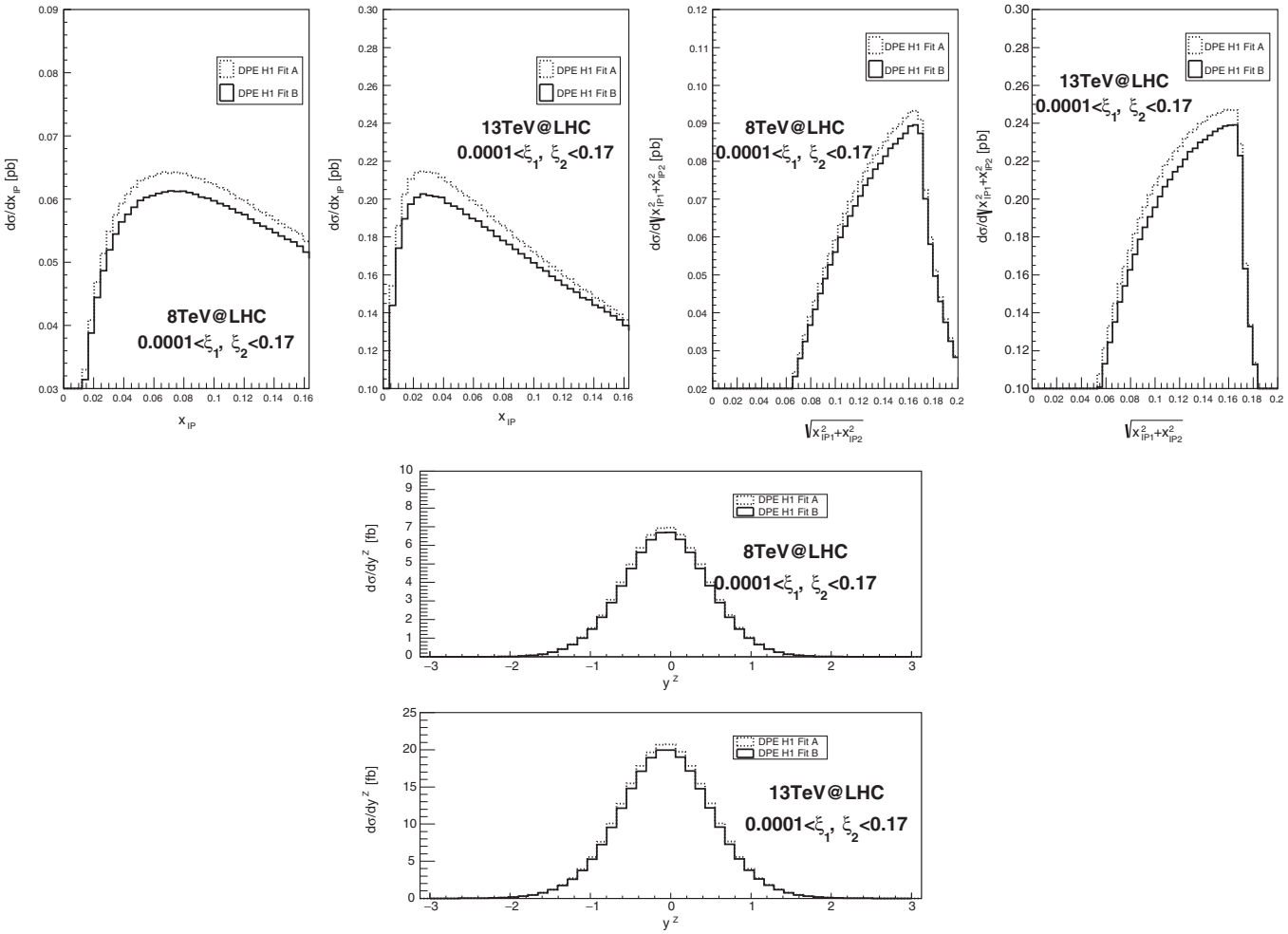

FIG. 7. Double Pomeron exchange (DPE) production of $x_{\mathbb{P}}$, $x'_{\mathbb{P}}$ and rapidity distributions at the 8 and 13 TeV LHC with the use of "H1 2006 dPDF Fit A" (solid curves) and "H1 2006 dPDF Fit B" (dotted curves). The detector acceptances are fixed in the range of $0.0001 < \xi_1 < 0.17$. Absorption effects are not included here.

1%–4% (3%–5%) for 7, 8 (13, 14) TeV correspondingly. For the double Pomeron exchange, the ratio R_2 varies in the range 0.03%–0.2% (0.1%–0.3%) for 7, 8 (13, 14) TeV, which are much smaller than that of R_1. By the definition of R parameters, predictions affected by large theoretical errors associated with scale variations can be reduced in a simple way. These predictions however does not take into account the gap survival suppression factor. In this respect, it would be still interesting to check whether the data follow at least the shape of the ratio as a function of M_{zz} as we shown in the future measurements.

Finally, in Fig. 9, we show the total cross sections (in unit of pb) for the single diffractive (SD) and double Pomeron exchange (DPE) cross sections, and compare to the photon-photon induced ($\gamma\gamma$) as well as nondiffractive (ND) Z-boson pair reactions, as a function of proton-proton CMS energy of 7, 8, 13 and 14 TeV at the LHC. We use solid, dashed, dotted and dash-dotted curves to present SD, DPE, $\gamma\gamma$ and ND cross sections, respectively. For SD, DPE and $\gamma\gamma$ production, both the detector acceptances of $0.0001 < \xi < 0.17$ (thin curve) and $0.015 < \xi < 0.15$ (thick curve) are considered. Notice here the rapidity gap survival probability factor is not taken into account. Features can been found in the figures and are listed as follows:

(i) The cross sections for different production mechanisms increase linearly as functions of the colliding energy.
(ii) Typical size order is normally $\sigma_{\rm ND} > \sigma_{\rm SD} > \sigma_{\rm DPE} > \sigma_{\gamma\gamma}$ as excepted.
(iii) Results from considering ATLAS-AFP detector acceptance ($0.015 < \xi < 0.15$) are comparable with that from TOTEM-CMS ($0.0001 < \xi < 0.17$) but a little smaller.

When the rapidity gap survival probability factor is considered, we can find that the SD cross section is at the order of $\sim\mathcal{O}(10\ \text{fb})$. For the DPE production rate is about 0.1–1 fb which is small but still larger than that of $\gamma\gamma$ induced production which is only about 0.1 fb. The

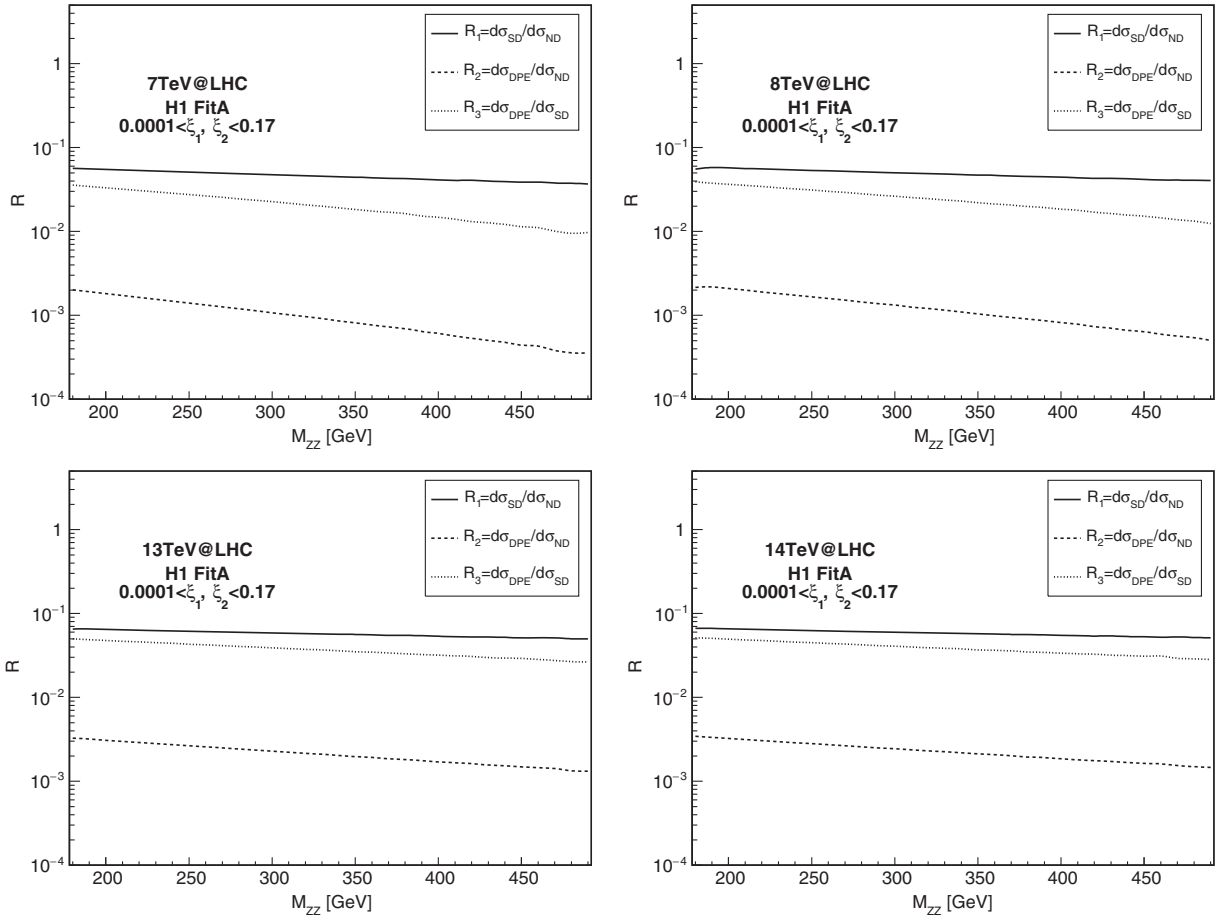

FIG. 8. R ratios as a function of the invariant mass M_{ZZ} for different values of the LHC energy. $0.0001 < \xi < 0.17$ for TOTEM-CMS is considered. Absorption effects are not included here.

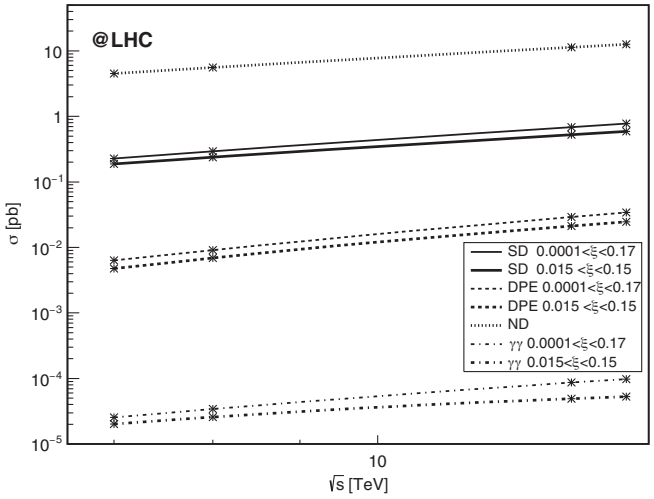

FIG. 9. The total cross sections (in unit of pb) for single diffractive (SD), double Pomeron exchange (DPE), photon-photon induced ($\gamma\gamma$) and nondiffractive (ND) Z-boson pair reactions as a function of proton-proton center-of-mass energy at the 7, 8, 13 and 14 TeV LHC. Both the detector acceptances of $0.0001 < \xi < 0.17$ and $0.015 < \xi < 0.15$ are considered. The rapidity gap survival probability factor is not taken into account here.

smallness of the Z-boson pair production, however, is not a thoroughly bad thing. As we said, when go to LHC energy frontier, exclusive production may open a new window to new physics searching [57,58], while in this case diffractive may serve as the important background. If a new sector is produced through gauge Z-boson pair production, such mechanism can be tested with a typical clean environment.

IV. CONCLUSION

A rich program at the Large Hadron Collider (LHC) is being pursued in diffractive physics by all collaborations either based on the identification of large rapidity gaps or the use of dedicated proton spectrometers. In our present study, we perform the calculation from the phenomenological analysis of Z-boson pair hard diffractive production at the LHC. Our calculation is based on the Regge factorization approach. Diffractive parton density functions (dPDFs) extracted by the H1 Collaboration at DESY-HERA are used and uncertainties by using different fits in the dPDFs are discussed. The multiple Pomeron exchange corrections are considered through the rapidity gap survival probability factor. We display various kinematical distributions for both the single diffractive(SD)

and double Pomeron exchange (DPE) productions. We give also numerical predictions for their cross sections and compare with the photon-induced and nondiffractive ones. The contributions from both quark-antiquark collision and gluon-gluon fusion modes are displayed and compared. We define the appropriate ratios of diffractive over nondiffractive (ND) productions, by using which predictions affected by theoretical errors associated with scale variations can be reduced. Typically the single diffractive ratio is varies between 5% and 7% while the double Pomeron exchange ratio varies in the range 0.03%–0.2% (0.1%–0.3%) for 7,8 (13, 14) TeV. We make predictions which could be compared to future measurements at the LHC where forward proton detectors are installed and detector acceptances are considered.

ACKNOWLEDGMENTS

This work is supported by the National Natural Science Foundation of China (Grant No. 11675033) and the Fundamental Research Funds for the Central Universities (Grant No. DUT15LK22).

[1] J. C. Collins, D. E. Soper, and G. F. Sterman, Factorization for short distance hadron-hadron scattering, Nucl. Phys. **B261**, 104 (1985).
[2] J. C. Collins, D. E. Soper, and G. F. Sterman, Soft gluons and factorization, Nucl. Phys. **B308**, 833 (1988).
[3] J. C. Collins, Proof of factorization for diffractive hard scattering, Phys. Rev. D **57**, 3051 (1998); Erratum, Phys. Rev. D **61**, 019092(E) (1999).
[4] G. Ingelman and P. E. Schlein, Jet structure in high mass diffractive scattering, Phys. Lett. B **152**, 256 (1985).
[5] F. D. Aaron *et al.* (ZEUS, H1 Collaboration), Combined inclusive diffractive cross sections measured with forward proton spectrometers in deep inelastic ep scattering at HERA, Eur. Phys. J. C **72**, 2175 (2012).
[6] J. D. Bjorken, Rapidity gaps and jets as a new-physics signature in very-high-energy hadron-hadron collisions, Phys. Rev. D **47**, 101 (1993).
[7] M. Albrow, P. Collins, and A. Penzo (CMS and LHCb Collaborations and FSC Team and HERSCHEL Team), Forward shower counters for diffractive physics at the LHC, Int. J. Mod. Phys. A **29**, 1446018 (2014).
[8] R. Schicker, Central exclusive production in the ALICE experiment at the LHC, Int. J. Mod. Phys. A **29**, 1446015 (2014).
[9] ATLAS Collaboration, CERN Reports No. CERN-LHCC-2011-012, No. LHCC-I-020 (to be published).
[10] M. Albrow *et al.*, CERN Reports No. CERN-LHCC-2014-021, No. TOTEM-TDR-003, No. CMS-TDR-13 (to be published).
[11] C. Royon and N. Cartiglia, The AFP and CT-PPS projects, Int. J. Mod. Phys. A **29**, 1446017 (2014).
[12] R. Fiore, L. Jenkovszky, and R. Schicker, Resonance production in Pomeron-Pomeron collisions at the LHC, Eur. Phys. J. C **76**, 38 (2016).
[13] L. L. Jenkovszky, O. E. Kuprash, J. W. Lamsa, V. K. Magas, and R. Orava, Dual-Regge approach to high-energy, low-mass diffraction dissociation, Phys. Rev. D **83**, 056014 (2011).
[14] L. Jenkovszky, O. Kuprash, R. Orava, and A. Salii, Low missing mass, single- and double diffraction dissociation at the LHC, Phys. At. Nucl. **77**, 1463 (2014).
[15] M. V. T. Machado, An estimation of single and double diffractive heavy flavour production in hadron-hadron colliders, Phys. Rev. D **76**, 054006 (2007).
[16] M. B. Gay Ducati, M. M. Machado, and M. V. T. Machado, Estimate of the single diffractive heavy quark production in heavy ion collisions at the CERN-LHC, Phys. Rev. D **81**, 054034 (2010).
[17] M. Heyssler, Diffractive heavy flavor production at the Tevatron and the LHC, Z. Phys. C **73**, 299 (1997).
[18] F. A. Ceccopieri, Single-diffractive Drell-Yan pair production at the LHC, Eur. Phys. J. C **77**, 56 (2017).
[19] C. Brenner Mariotto and V. P. Goncalves, Diffractive photon production at the LHC, Phys. Rev. D **88**, 074023 (2013).
[20] M. Heyssler, Z. Kunszt, and W. James Stirling, Diffractive Higgs production at the LHC, Phys. Lett. B **406**, 95 (1997).
[21] M. B. Gay Ducati, M. M. Machado, and G. G. Silveira, Estimations for the single diffractive production of the Higgs boson at the Tevatron and the LHC, Phys. Rev. D **83**, 074005 (2011).
[22] R. Enberg, G. Ingelman, and N. Timneanu, Diffractive Higgs and prompt photons at hadron colliders, Phys. Rev. D **67**, 011301 (2003).
[23] S. Erhan, V. T. Kim, and P. E. Schlein, Reports No. CERN-TH-2003-232, No. UCLA-EPP-2003-101.
[24] M. Tasevsky, Review of central exclusive production of the Higgs boson beyond the Standard Model, Int. J. Mod. Phys. A **29**, 1446012 (2014).
[25] M. Tasevsky, Exclusive MSSM Higgs production at the LHC after Run I, Eur. Phys. J. C **73**, 2672 (2013).
[26] F. Abe *et al.* (CDF Collaboration), Observation of Diffractive W-Boson Production at the Tevatron, Phys. Rev. Lett. **78**, 2698 (1997).
[27] P. Bruni and G. Ingelman, Diffractive W and Z production at pp colliders and the pomeron parton content, Phys. Lett. B **311**, 317 (1993).
[28] L. Alvero, J. C. Collins, J. Terron, and J. J. Whitmore, Diffractive production of jets and weak bosons, and tests of hard scattering factorization, Phys. Rev. D **59**, 074022 (1999).
[29] R. J. M. Covolan and M. S. Soares, Analysis on the diffractive production of W's and dijets at the DESY HERA and Fermilab Tevatron colliders, Phys. Rev. D **60**, 054005 (1999); Erratum, Phys. Rev. D **61**, 019901(E) (1999).

[30] R. J. M. Covolan and M. S. Soares, Diffractive hadroproduction of dijets and W's at the Tevatron collider and the pomeron structure function, Phys. Rev. D **67**, 017503 (2003).
[31] R. Pasechnik, B. Kopeliovich, and I. Potashnikova, Diffractive gauge bosons production beyond QCD factorization, Phys. Rev. D **86**, 114039 (2012).
[32] M. B. Gay Ducati, M. M. Machado, and M. V. T. Machado, Diffractive hadroproduction of W, and Z bosons at high energies, Phys. Rev. D **75**, 114013 (2007).
[33] K. Golec-Biernat and A. Luszczak, Diffractive production of electroweak vector bosons at the LHC, Phys. Rev. D **81**, 014009 (2010).
[34] E. Basso, V. P. Goncalves, and M. S. Rangel, Probing the diffractive production of gauge bosons at forward rapidities, Eur. Phys. J. C **76**, 689 (2016).
[35] G. Ingelman, R. Pasechnik, J. Rathsman, and D. Werder, Diffractive $W^{\pm}$ production at hadron colliders as a test of colour singlet exchange mechanisms, Phys. Rev. D **87**, 094017 (2013).
[36] M. Luszczak, A. Szczurek, and C. Royon, W^+W^- pair production in proton-proton collisions: small missing terms, J. High Energy Phys. 02 (2015) 098.
[37] P. Lebiedowicz, R. Pasechnik, and A. Szczurek, QCD diffractive mechanism of exclusive W^+W^- pair production at high energies, Nucl. Phys. **B867**, 61 (2013).
[38] A. Aktas *et al.* (H1 Collaboration), Measurement and QCD analysis of the diffractive deep-inelastic scattering cross section at HERA, Eur. Phys. J. C **48**, 715 (2006).
[39] P. D. B. Collins, *An Introduction to Regge Theory and High Energy Physics* (Cambridge University Press, Cambridge, England, 1977).
[40] A. Donnachie and P. V. Landshoff, Diffractive deep inelastic lepton scattering, Phys. Lett. B **191**, 309 (1987); Erratum, Phys. Lett. B **198**, 590(E) (1987).
[41] A. Donnachie and P. V. Landshoff, Hard diffraction: Production of high p_T jets, W or Z, and Drell-Yan pairs, Nucl. Phys. **B303**, 634 (1988).
[42] A. Aktas *et al.*, H1 collaboration, diffractive deep-inelastic scattering with a leading proton at HERA, DESY 06-048, Eur. Phys. J. C **48**, 749 (2006).
[43] A. Cisek, W. Schafer, and A. Szczurek, Production of Z^0 bosons with rapidity gaps: Exclusive photoproduction in γp and pp collisions and inclusive double diffractive Z^0's, Phys. Rev. D **80**, 074013 (2009).
[44] V. A. Khoze, A. D. Martin, and M. G. Ryskin, Soft diffraction and the elastic slope at Tevatron and LHC energies: A multi-Pomeron approach, Eur. Phys. J. C **18**, 167 (2000).
[45] U. Maor, The interplay between data and theory in recent unitarity models, AIP Conf. Proc. **1105**, 248 (2009).
[46] CMS Collaboration, Observation of a diffractive contribution to dijet production in proton-proton collisions at $\sqrt{s} = 7$ TeV, Phys. Rev. D **87**, 012006 (2013).
[47] M. Trzebiński, Machine optics studies for the LHC measurements, Proc. SPIE Int. Soc. Opt. Eng. **9290**, 929026 (2014).
[48] A. K. Kohara and C. Marquet, Prompt photon production in double-Pomeron-exchange events at the LHC, Phys. Lett. B **757**, 393 (2016).
[49] T. Hahn, Generating Feynman diagrams and amplitudes with FeynArts 3, Comput. Phys. Commun. **140**, 418 (2001).
[50] T. Hahn, Automatic loop calculations with FeynArts, FormCalc, and LoopTools, Nucl. Phys. B, Proc. Suppl. **89**, 231 (2000); S. Agrawal, T. Hahn, and E. Mirabella, FormCalc 7, J. Phys. Conf. Ser. **368**, 012054 (2012).
[51] T. Hahn and M. Perez-Victoria, Automatized one loop calculations in four-dimensions and D-dimensions, Comput. Phys. Commun. **118**, 153 (1999).
[52] S. Kawabata, A new version of the multi-dimensional integration and event generation package BASES/SPRING, Comput. Phys. Commun. **88**, 309 (1995); F. Yuasa, D. Perret-Gallix, S. Kawabata, and T. Ishikawa, PVM-GRACE, Nucl. Instrum. Methods Phys. Res., Sect. A **389**, 77 (1997).
[53] J. Pumplin, D. R. Stump, J. Huston, H. L. Lai, P. M. Nadolsky, and W. K. Tung, New generation of parton distributions with uncertainties from global QCD analysis, J. High Energy Phys. 07 (2002) 012; D. Stump, J. Huston, J. Pumplin, W.-K. Tung, H. L. Lai, S. Kuhlmann, and J. F. Owens, Inclusive jet production, parton distributions, and the search for new physics, J. High Energy Phys. 10 (2003) 046.
[54] T. Affolder *et al.* (CDF Collaboration), Observation of Diffractive Beauty Production at the Fermilab Tevatron, Phys. Rev. Lett. **84**, 232 (2000).
[55] T. Aaltonen *et al.* (CDF Collaboration), Diffractive W and Z production at the Fermilab Tevatron, Phys. Rev. D **82**, 112004 (2010).
[56] T. Aaltonen *et al.* (CDF Collaboration), Diffractive dijet production in $\bar{p}p$ collisions at $\sqrt{s} = 1.96$ TeV, Phys. Rev. D **86**, 032009 (2012).
[57] R. S. Gupta, Probing quartic neutral gauge boson couplings using diffractive photon fusion at the LHC, Phys. Rev. D **85**, 014006 (2012).
[58] E. Chapon, O. Kepka, and C. Royon, Anomalous quartic $WW\gamma\gamma$, $ZZ\gamma\gamma$, and trilinear $WW\gamma$ couplings in two-photon processes at high luminosity at the LHC, Phys. Rev. D **81**, 074003 (2010).